A general mechanism for the meandering of rivulets

A. Daerr[1], J. Eggers[2], L. Limat[1], and N. Valade[1]
[1] *Laboratoire Matière et Systèmes Complexes, UMR 7057 of CNRS and University Paris Diderot, 10 rue Alice Domon et Léonie Duquet, 75025 Paris Cedex 13, France,*
[2] *School of Mathematics, University of Bristol, Bristol BS8 1TW, United Kingdom*

A rivulet flowing down an inclined plane often does not follow a straight path, but starts to meander spontaneously. Here we show that this instability is the result of two key ingredients: fluid inertia and anisotropy of the friction between rivulet and substrate. Meandering only occurs if the motion normal to the instantaneous flow direction is more difficult than parallel to it. We give a quantitative criterion for the onset of meandering, and confirm it by comparing to the flow of a rivulet between to glass plates which are wetted completely. Above the threshold, the rivulet follows an irregular pattern with a typical wavelength of a few cm.

Meandering of rivulets down a vertical or inclined surface is a well known phenomenon [1–10], which is a fundamental ingredient to our understanding of flow over solid surfaces. For example, the meandering pattern determines the degree to which a solid surface is covered by a liquid film: the width of a rivulet may be 1mm, while the transversal excursions of a meander may be several cm. The small-scale meanders discussed in this paper also fall into a broader class of instabilities which include river meandering [11], and which are related to problems of statistical physics [4]. Most explanations of meandering are based on the idea that centrifugal forces amplify the curved parts of the stream [1, 4, 8], while others emphasize the role of noise and surface disorder [9, 10]. However, as yet there exists no quantitative theory of meandering; indeed, it is unclear how centrifugal forces can generate instability. A straight rivulet appears to be more favorable than a curved one, both from a point of view of an inertial mass, as well as from considerations of surface energy.

Most available experiments were performed in partial wetting conditions, and on relatively rough substrates, which suffer from contact angle hysteresis, and the pinning of the rivulet on defects. Thus the mechanism of instability remains hidden by noise, and quantitative comparison is difficult. Instead, we have performed meandering experiments in a situation of complete wetting, where hysteresis and surface defects do not matter. To this end we confined a fluid with low surface tension (silicone oil) between two parallel plates (the Hele-Shaw geometry), so a rivulet forms as a long liquid bridge or film connecting the two plates, see Fig. 1. The insides of the glass plates are covered with a thin fluid film, since the silicone oil strongly favors wetting. Previous meandering experiments in the same geometry have only been reported with a surfactant aiding the stability of the bridge [3, 12]. This makes the results difficult to reproduce, and poses questions as to the role of complex surfactant rheology.

In the present letter, we show that a meandering instability exists for an inert, Newtonian fluid (silicone oil) between two glass plates, thus establishing its universal nature. By varying the flow rate, we show that the rivulet meanders above a well-defined threshold. Based on a hydrodynamic description, we derive an explicit and parameter-free criterion for the threshold value of the critical flow speed above which meandering occurs. We observe that the one crucial ingredient necessary for meandering is that it is harder for the fluid to move in a direction perpendicular to the instantaneous direction of the rivulet, than it is to move in a downstream direction. Paradoxically, in such a situation inertia tends to move the rivulet in the transversal direction, against the energetically favored state.

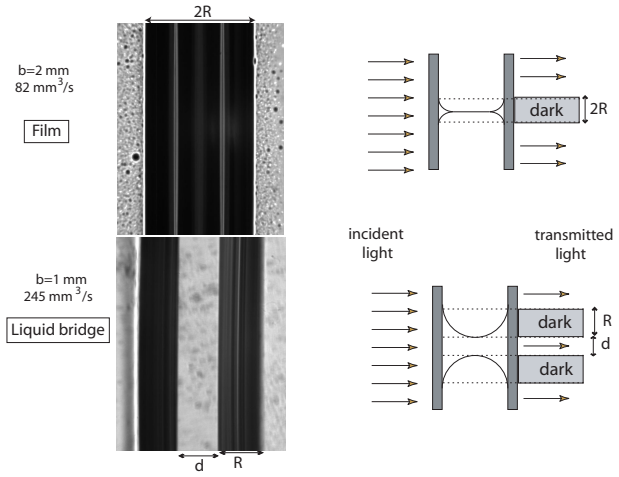


FIG. 1: Silicone oil forms a rivulet between two glass plates, whose cross section can either be a film (top) or a liquid bridge (bottom). Dimensions are R=0.7mm at the top, and R=0.5mm at the bottom. On the left, closeup frontal views of the glass plates, used to measure the rivulet width. On the right, a schematic of the rivulet as it would appear from the side. At low flow rates and large plate separations b, a film forms (top); the rivulet is imaged as a single black line, and the cross-sectional area is $A = (4-\pi)R^2$. At higher flow rates or small separation, a liquid bridge appears (bottom), imaged as a bright line bounded by two black lines. The area is $A = (4-\pi)R^2 + bd$.

Our experiment consists of a Hele-Shaw cell made of two glass plates of dimensions 100 cm x 30 cm and thick-

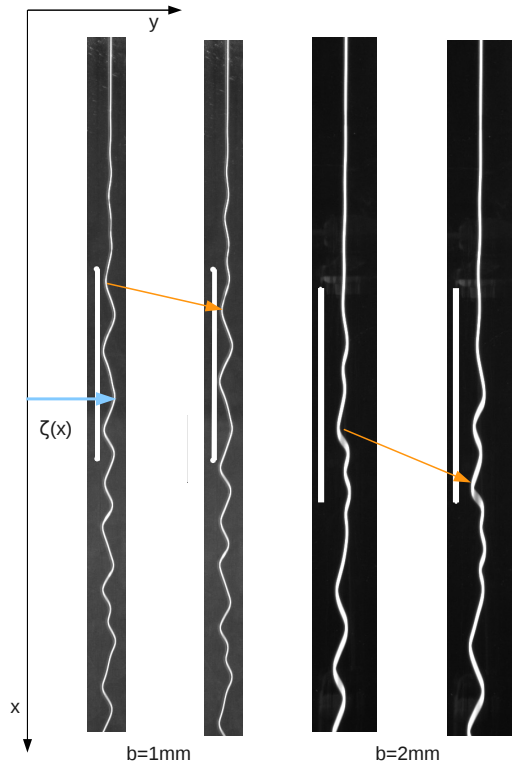


FIG. 2: Typical meandering patterns obtained with silicone oil of viscosity 3 cP, at flow rates $Q = 182mm^3/s$ (left) and $Q = 347mm^3/s$ (right), slightly above the threshold. The scale bar is 10 cm long. Shown are two successive images with $\Delta t = 0.33$ s between them. The spatial shift, indicated by an arrow, shows the phase velocity $u_\phi = 2.95$ cm/s (left) and 2.42 cm/s (right). Note the irregularity of the pattern.

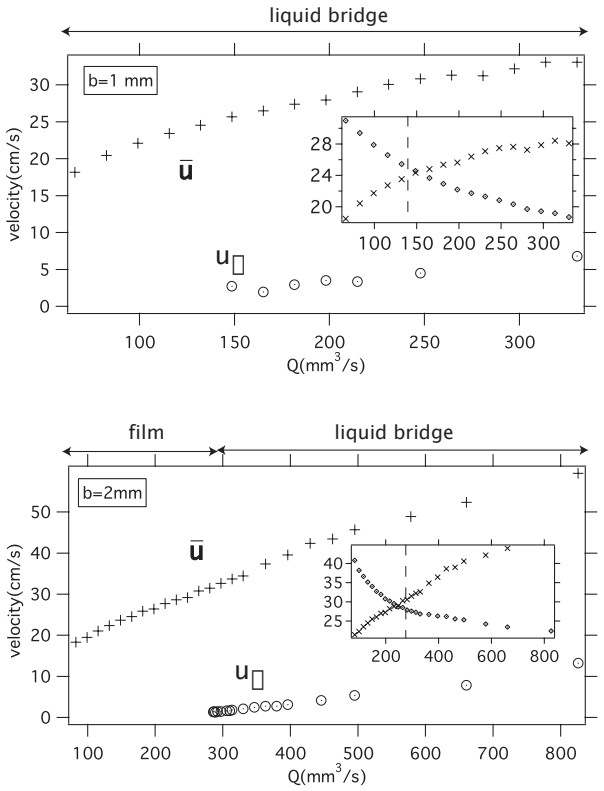


FIG. 3: The mean velocity (+) and phase velocity (○) as function of the flow rate, for the two plate spacings of b= 1 mm and 2mm. The insets show $\bar{u} - u_\phi$ (x), (u_ϕ being calculated from a linear approximation to the data) and $\sqrt{\Gamma}$ (◇), which should cross at the threshold. The vertical line is the observed threshold. For our silicone oil $\gamma/\rho = 22cm^3/s^2$, and A is calculated from the measured values of R and d, see Fig. 1.

ness 5 mm, arranged vertically. The gap between the plates is maintained by spacers; we report the results of two series of experiments, one with a plate separation of b=1mm, the other with b=2mm. A gear pump injects silicone oil 3 times as viscous as water (3 cP) at the top of a cell through a hypodermic needle; typical flow rates lie between 50 and 1000 mm^3/s. The shape assumed by the rivulet in the plane of the cell is followed by video recording, the cell being lit by a long Neon tube placed two meters behind it. Closeup views (see Fig. 1) are used to measure the width of the rivulet and thus its cross section. Depending on the flow rate relative to plate spacing, two different states are observed. At low flow rates, a thin liquid film, connected to the plate through Plateau borders, which shows up as a single dark line. At higher flow rates, a liquid bridge, which appears as a bright line with dark borders (cf. Fig. 1).

At low flow rates, the rivulet remains perfectly straight over the whole length of the Hele Shaw cell. Moreover, its width stays constant over the whole length of the cell, indicating that the flow is fully developed from near the inlet, and the mean flow speed is determined by a balance of gravity and viscous friction. Above a critical flow rate, irregular meandering patterns begin to develop, which are convected downstream, as shown in Fig.2. Typical wavelengths are of the order of a few cm, much larger that the rivulet width of a few mm. The phase velocity u_ϕ of the meandering pattern is illustrated using two images with a time delay of 0.33 s between them.

In Fig. 3 we have plotted the mean velocity $\bar{u}$ of the flow inside the rivulet, and the phase velocity u_ϕ of the meandering pattern, for two different plate spacings. Though the meanders are convected downstream by the flow, their drift velocity (i.e. phase velocity) is nearly five times smaller than the fluid velocity itself, which suggests that motion normal to the rivulet is inhibited. The mean velocity is calculated from $\bar{u} = Q/A$, where the cross-

sectional area A is calculated according to the diagrams in Fig. 1 (see caption). In the film regime, we measure the width $2R$ of the dark line, where R is the radius of curvature of the Plateau border, and $b-2R$ the length of the film. In the liquid bridge regime we measure the width d of the bright line as well as the width R of the dark borders, which is now the radius of curvature of the meniscus bordering the bridge. All surfaces are assumed to be arcs of circles, forming 180° contact angles everywhere. The phase velocity u_ϕ is determined from a linear fit to the spatio-temporal plot of the meandering pattern. We will now show that the parameter controlling stability is the difference $\Delta u = \bar{u} - u_\phi$.

To explain the observed instability theoretically, we use the two-dimensional Navier-Stokes equation, as obtained from averaging the flow in the z-direction (parallel to the plates), as customary for Hele-Shaw flow [13]. The velocity field is $\mathbf{u} = (u, v)$, where the first, x-component is taken down the incline (cf. Fig.2):

$$\partial_t \mathbf{u} + (\mathbf{u}\cdot\nabla)\mathbf{u} = -k\mathbf{u} + (\Gamma\kappa - k_{cl}u_n)\mathbf{n} + g\mathbf{e}_x. \qquad (1)$$

The friction factor is $k = 12\nu/b^2$ for Poiseuille flow (ν the kinematic viscosity), but with different prefactors for the slightly more complicated rivulet geometries shown in Fig. 1. In general, there also appears a prefactor β in front of the convective term, which is $\beta = 6/5$ for Poiseuille flow [13, 14]. We disregard it here for simplicity, as we are able to write the final result for the threshold in a parameter-free from, independent of β.

Because of the contact line between the rivulet and the liquid film covering the plates (cf. Fig. 1), there is an additional friction factor that depends only on the speed of the rivulet normal to its orientation. We are not aware of k_{cl} having been calculated before in the limit of small speeds of interest here; the nonlinear law given in [15] only applies for speeds such that the thickness of the corresponding "Landau-Levich-Derjaguin" film [16] is greater than the pre-existing one. We will avoid calculating k_{cl} by relating it to the phase velocity of the meandering pattern, which can be measured experimentally.

A second contribution to the normal force comes from the curvature κ of the rivulet, since a curved rivulet has a greater surface area. In the case of a liquid bridge of finite width (cf. Fig. 1 (bottom)), it was shown in [15] that the pressure difference across the meniscus in the small-speed limit is $\Delta p = -\gamma\pi\kappa/4$. This leads to $\Gamma = \gamma\pi b/(2\rho A)$ in (1), which contains a factor of 2, to account for the 2 sides of the rivulet. Here γ the surface tension, and ρ the density of the fluid. In the film regime the interface is planar over a length $b-2R$, which contributes a factor $\Gamma = 2\gamma(b-2R)/(\rho A)$, the other part is curved with a radius of curvature R (cf. Fig. 1 (top)). A combination of the contribution of both curved and straight interfaces gives the generalized formula $\Gamma = \gamma(2(b-2R) + R\pi)/(\rho A)$.

We now perform a linear stability analysis of (1), assuming small deviations of the rivulet position $\zeta(x)$ from the vertical (cf. Fig. 2). For u, we can take the mean velocity $\bar{u} = g/k$, so (1) becomes:

$$\zeta_t + \bar{u}\zeta_x = v \qquad (2)$$

$$v_t + \bar{u}v_x = -kv - k_{cl}u_n + \Gamma\zeta_{xx}, \qquad (3)$$

with subscripts denoting partial differentiation. Here (2) describes the convection of the rivulet by the flow, and (3) is the y-component of the Navier-Stokes equation (1). The normal velocity of the rivulet is related to the velocity $(\bar{u}, v)$ relative to the plate by $u_n = v - \bar{u}\zeta_x$. Using the first equation, the variable v can be eliminated everywhere, leading to

$$\zeta_{tt} + 2\bar{u}\zeta_{xt} + \bar{u}^2\zeta_{xx} = -(k+k_{cl})\zeta_t - k\bar{u}\zeta_x + \Gamma\zeta_{xx}. \qquad (4)$$

Note that the $\bar{u}^2$-term stands for centrifugal forces such as those invoked in [1, 2, 8, 12], but it is important to realize that inertia by itself does not lead to instability. To illustrate this, let us consider an ideal case in which the right hand side of (4) is negligible. If one seeks solutions of the form $\zeta(x,t) \propto \exp(iqx + \sigma t)$, the dispersion relation reduces to $\sigma = -iq\bar{u}$, i.e. there is only propagation without amplification, with a phase velocity equal to the liquid velocity. If one includes frictional terms proportional to k as well as surface tension forces, this only leads to damping of an initially excited wave.

However, the full dispersion relation for (4) reads

$$\sigma = -iq\bar{u} - \bar{k} \pm \sqrt{-\Gamma q^2 + \bar{k}^2 + ik_{cl}\bar{u}q}, \qquad (5)$$

where $\bar{k} = (k + k_{cl})/2$. It is confirmed easily that the second branch is always damped, while the first becomes unstable if

$$k_{cl}^2\bar{u}^2 > 4\bar{k}^2\Gamma, \qquad (6)$$

i.e. when centrifugal forces overwhelm surface tension. The physical mechanism behind the instability now becomes clear, by comparing to the result for an unconstrained rivulet. According to Galileo, a free mass will always continue in a straight line, perhaps being slowed down by frictional forces along the way. For centrifugal forces to come into play, and thus to cause instability, there must be a *constraint* on the motion. But such a constraint exists only if there is a supplementary friction term k_{cl}, which singles out the momentary shape of the rivulet as a preferred path. As is apparent from (6), no instability occurs if k_{cl} is set to zero.

This idea can be expressed more formally by observing that at the threshold, the dispersion becomes $\sigma = -i\bar{u}qk/(2\bar{k})$, thus the meandering pattern moves with a phase velocity

$$u_\phi = \frac{k}{2\bar{k}}\bar{u}. \qquad (7)$$

This permits to put the stability criterion (6) into a parameter-free from:

$$(\bar{u} - u_\phi)^2 > \Gamma, \tag{8}$$

which is the main result of this paper. This condition expresses the physical essence of our mechanism: $\Delta u = \bar{u} - u_\phi$ is the speed of a fluid particle in the frame of reference of the pattern in which it moves; it is this difference only which results in centrifugal forces on the structure. Note that the substantial difference between $\bar{u}$ and u_ϕ, evident in Fig. 3, results from the fact that the inclined parts of the stream are slowing down the motion of the meandering pattern, because of the extra resistance to normal motion of the contact line, a fact expressed mathematically by (7). This idea is equivalent to the notion of a "constraint" imposed on the motion, as explained above.

We are now in a position to test our theory quantitatively, without being required to know the friction coefficients k and k_{cl} quantitatively, and without adjustment of parameters. The contact line friction, in particular, is difficult to determine since we do not know the thickness of the deposited film. Its thickness will be determined both by drainige of the film, as well as (at least in the unstable regime) the dynamics of the rivulet sweeping over the plates. In the inset of Fig. 3, we have plotted Δu and $\sqrt{\Gamma}$, which according to (8) should cross at the transition; the meandering transition observed by us experimentally is marked by a vertical line, which indeed coincides well with the crossing of the two curves (insets in Fig. 3).

However, one aspect we do not yet understand is the selection of a typical wavelength, as illustrated in Fig. 2. Above the threshold, (5) predicts all wavelengths to turn unstable at the same time, since there is no maximum in the dispersion relation which would select a most unstable wavelength. One physical effect we have not yet taken into account is the regularization at short wavelengths, which are of the order of the width of the rivulet. However, this will not explain the observed wavelengths, which are much larger than the rivulet width. Rather, we suspect that selection occurs on account of a nonlinear mechanism. This is consistent with the irregular appearance of meanders, whose shape is quite far from sinusoidal, and which exhibit a very considerable spread in wavelength.

In conclusion, we have presented a theory for the meandering of rivulets, which agrees quantitatively with experiment. While large-scale meandering, for example of rivers, is governed by very different mechanisms, we believe nonetheless that the basic physical principle behind the instability is the same as the one described by us. On one hand, the driving force ultimately comes from the inertia of the fluid. On the other hand, for this force to act one needs a reference frame, which in the case of rivers is furnished by the existence of a river bed.

A. D. and L.L. are indebted to B. Andreotti, W. Drenkhan, and F. Elias, for stimulating discussions at the begining of this project.

[1] J. B. Culkin and S. H. Davis, AIChE J. **30**, 263 (1984).
[2] T. Nakagawa and J. C. Scott, J. Fluid. Mech. **149**, 89 (1984).
[3] A. Anand and A. Bejan, J. Fluids Eng. **108**, 269 (1986).
[4] R. Bruinsma, J. Phys. (France) **51**, 829 (1990).
[5] P. Schmuki and M. Laso, J. Fluid Mech. **215**, 125 (1990).
[6] T. Nakagawa, J. Multiphase Flow **18**, 455 (1992).
[7] H. Kim, J. Kim, and B. Kang, J. Fluid. Mech. **498**, 245 (2004).
[8] N. Le Grand, A. Daerr, and L. Limat, Phys. Rev. Lett. **96**, 254503 (2006).
[9] B. Birnir, K. Mertens, V. Putkaradze, and P. Vorobieff, J. Fluid Mech. **607**, 401 (2008).
[10] B. Birnir, K. Mertens, V. Putkaradze, and P. Vorobieff, Phys. Rev. Lett. **101**, 114501 (2008).
[11] L. B. Leopold and M. G. Wolman, Geol. Soc. Am. Bull. **71**, 769 (1960).
[12] W. Drenkhan, S. Gatz, and D. Weaire, Phys. Fluids **16**, 3115 (2004).
[13] F. Plouraboué and E. J. Hinch, Phys. Fluids **14**, 922 (2002).
[14] C. Ruyer-Quil, C. R. Acad. Sci., Ser. IIb: Mec., Phys., Chim., Astron. **329**, 1 (2001).
[15] C.-W. Park and G. M. Homsy, J. Fluid Mech. **139**, 291 (1984).
[16] J. H. Snoeijer, J. Ziegler, B. Andreotti, M. Fermigier, and J. Eggers, Phys. Rev. Lett. **100**, 244502 (2008).